^{19}F spectroscopy and relaxation behavior of trifluorovinyldichloroborane

W.J. Boyko,[a] R.L. Dudley,[b] G.F. Kemmerer,[c] and A.J. Leffler[d,*]

[a] Department of Chemistry, Villanova University, Villanova, PA 19085, USA
[b] Eastern Regional Research Center, US Department of Agriculture, Wyndmoor, PA 19038, USA
[c] Department of Chemistry, Temple University, Philadelphia, PA 19122, USA
[d] Department of Physics, Bryn Mawr College, Bryn Mawr, PA 19010, USA

Abstract

The ^{19}F NMR spectra and spin–lattice relaxation rate, R_1, of trifluorovinyldichloroborane as shown in Fig. 2 were studied as a function of temperature, T, and magnetic field, B. All $\log R_1$ vs $1/T$ plots show a minimum at 299 K indicating the presence if dipolar relaxation at lower T and spin–rotation relaxation at higher T. The R_1 values increase with increasing B due to chemical shift anisotropy relaxation. Estimates of the fluorine chemical shift values for F_3 (cf. Fig. 1) suggest that there is π character in the F–C bond. The other two C–F bonds are largely single bonded. No evidence was found for intermolecular exchange of the trifluorovinyl group. Two of the three fluorine atoms show large increases in their NMR linewidth with increasing temperature while the third shows only a small increase but the activation energy for the process is the same for all. The increase in linewidths is due to scalar coupling to the boron atoms. The boron linewidths were measured between 253 and 363 K and decreased with increasing temperature. A plot of $\log R_2$, where R_2 is the linewidth of the boron as a function of $1/T$ shows some curvature indicating a second relaxation mechanism. This is ascribed to spin–rotation but not enough data are available to be conclusive. In all cases there is a second small set of fluorine peaks that are due to ^{10}B interactions separated from the ^{11}B peaks by amounts varying from 1 to 4 ppm depending on the field and fluorine atom.
© 2003 Elsevier Inc. All rights reserved.

1. Introduction

In previous studies of the ^{19}F NMR spectra of a series of metalloorganic compounds containing the trifluorovinyl group by Kaesz et al. [1] and Coyle et al. [2] it was noted that the boron containing compounds differed from the others because they had unusually broad linewidths at ambient temperature. These boron compounds were different from the remainder synthesized because they were the only ones containing a Group III element while the others contained Group XIV elements. It has been shown [3] that the acidity of the $C_2F_3BCl_2$ molecule falls between the BF_3 and BCl_3, indicating that the electron withdrawing ability of the trifluorovinyl group falls between that of F and Cl. Based on accepted bonding arguments [4] this would indicate that there is multiple bonding between boron and the adjacent carbon atom in each of these molecules.

Using the numbering scheme of Coyle et al. [2], shown in Fig. 1, the F_3 atom bonded to the carbon atom adjacent to the boron atom shows a pair of peaks while the F_1 diagonal to the boron atom gives a single broad line at ambient temperature. The original workers explained these results qualitatively as broadenings due to boron quadrupolar effects. Advances in high field NMR now allow for a more thorough study of the fluorine line broadenings and multiple bonding of these compounds.

2. Experimental

2.1. Materials

Trifluorovinlydichloroborane was prepared by the method described in the literature [1]. This type of boron compounds is extremely sensitive to moisture and oxidation, actually exploding in the presence of oxygen. Bis(trifluorovinyl)chloroborane is very unstable to disproportionation to the mono and tris trifluorovinyl
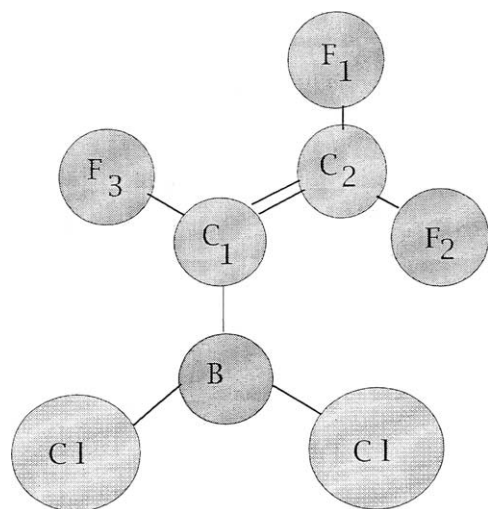

Fig. 1. Molecular structure and atom numbering for trifluorovinyldichloroborane. The assumed bond distances are in Å, B–Cl 1.761, B–C 1.59, C_1–C_2, all C–F 1.33.

compounds and has never been isolated in pure form. The tris compound is difficult to prepare using the original procedure due to polymerization from the heat of reaction but can be made by diluting the reaction mixture of BCl_3 and $(C_2F_3)_2SnCl_2$ with an inert solvent such as Freon E-5.

2.2. NMR measurements

The sample for study was sealed in a 5 mm NMR tube together with a small amount of boron trichloride and perdeuterotoluene as the lock solvent. The added boron trichloride was designed to minimize any disproportionation of the trifluorovinlydichloroborane. It was noted during the spectral measurements up to the highest temperatures used that the chemical shifts of both boron compounds remained nearly constant indicating no intermolecular exchange.

All ^{19}F spectra were obtained between −70 and 90 °C using Varian XL-200, Varian Unity$^+$ 400, and GE 500 MHz spectrometers. Some of the spectra taken at 200 MHz are shown in Figs. 3–5. In addition ^{11}B measurements were made at 64 MHz from −20 to 90 °C and one at ambient temperature at 164 MHz. Linewidth measurements were made at half height while R_1 measurements were performed using the standard $180–\tau–90°$ pulse sequence. All calculations of R_1 were carried out using spectrometer software.

3. Results

3.1. Spin–lattice relaxation

For any spin in a molecule the observed nuclear spin–lattice relaxation rate, $(R_1)_{observ}$ is taken to be the sum of the longitudinal relaxation rates of each operative mechanism:

$$(R_1)_{observ} = (R_1)_{dd} + (R_1)_{CSA} + (R_1)_{sr}, \qquad (1)$$

where $(R_1)_{dd}$ is the dipolar, $(R_1)_{CSA}$ is the chemical shift anisotropy, and $(R_1)_{sr}$ is the spin–rotation. In the present work the aim is to separate the various mechanisms using observations of R_1 of the three chemically inequivalent fluorines at three different field strengths over a temperature range of 160°. Similar separation difficulties have been found in earlier studies of $PbCl_4$ and other molecules [5]. The boron spectra over a portion of this temperature range show no change in chemical shift between BCl_3 and $C_2F_3BCl_2$ indicating no chemical exchange. In Fig. 2 the observed value of R_1 values for F_1 are shown on a logarithmic scale versus T^{-1} together with fits of the data using cubic least squares plots through each the points. This is only a convenient parameterization of the data and has no theoretical basis. No error bars are shown due to the closeness of the curves but it is estimated that R_1 values are accurate to ±10%. Similar plots not shown were made for the other fluorine atoms.

The chemical shift anisotropy values were obtained using the method of Hawk and Sharp [5]. We rewrite (1) as

$$(R_1)_{observ} = (R_1)_{CSA} + (R_1)_{otherv} \qquad (2)$$

for each field, where $(R_1)_{otherv}$ are the remaining independent terms in (1). Since the chemical shift anisotropy relaxation is proportional to the square of the external field, CSA values at any two fields are related by:

$$(R_1)_{B1CSA} = (B_1/B_2)^2 (R_1)_{B2CSA}, \qquad (3)$$

where the B's are the field values. Thus (2) can be written for two fields and the $(R_1)_{CSA}$ values related through (3) giving:

$$(R_1)_{B1observ} - (R_2)_{B1observ} = \left((R_1)_{B2CSA}(B_1/B_2)^2 - 1 \right)$$

$$\qquad (4)$$

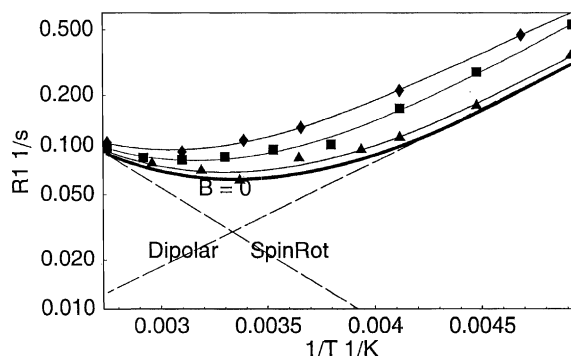Fig. 2. ^{19}F log(R_1), for F_1 vs T^{-1}. Values are shown for 188 MHz (◆), 376 MHz (■), 470 MHz (▲), and the calculated R_1 for $B = 0$. Also shown are calculated values of the $(R_1)_{dd}$ and $(R_1)_{CSA}$ as discussed in the text. The three full lines are cubic least square fits.

and then can be rearranged to:

$$(R_1)_{\text{B2CSA}} = [(R_1)_{\text{B1observ}} - (R_2)_{\text{B1observ}}][(B_1/B_2)^2 - 1] \quad (5)$$

with corresponding equations for each $(R_1)_{\text{B}i\text{CSA}}$ ($i = 1, 2, 3$) of the other fields. In the present work there were observations at three fields and therefore two $(R_1)_{\text{B}i\text{CSA}}$ values for each field could be calculated. The average of each of these three sets of data was used because they varied by about 20%. Subtraction of $(R_1)_{\text{observ}} - (R_1)_{\text{CSA}}$ at each field for each temperature gave almost the same values for $(R_1)_{\text{otherv}}$ as expected from (2) and the resultant curve is shown in Fig. 2 as the $B = 0$ field value. Similar results were obtained for the other two fluorine atoms.

$(R_1)_{\text{otherv}}$ vs T^{-1} is field independent as expected while a minimum for R_1 indicates the presence of at least two mechanisms. The exchange mechanism has been ruled out by the boron spectra and scalar coupling is very small for $(R_1)_{\text{otherv}}$ as discussed below, leaving dipolar and spin–rotation as the operative mechanisms. It is possible to separate the contributions of each mechanism to the total relaxation by assuming that at low temperatures the dipolar mechanism is dominant while at high temperatures only the spin–rotation is significant. At any observed temperature the observed $(R_1)_{\text{otherv}}$ value is the sum of the contributions from each operative mechanism as shown in Eq. (1). In the case where the line slopes differ only by a sign and when the $(R_1)_{\text{otherv}}$ curve is a minimum, each mechanism contributes one half of the observed R_1 value. A plot of $\log(R_1)_{\text{dd}}$ as a function of T^{-1} is assumed to be a straight line through the values at the lowest temperatures for $1/2(R_1)_{\text{other, min}}$. The dipolar relaxation, $(R_1)_{\text{dd}}$, values for all temperatures may be obtained by subtracting the dipolar values from the R_1 values at zero field. The results are shown in Fig. 2.

3.2. Spin–spin relaxation

The peak shapes shown in Figs. 3–5 were simulated by the relation obtained using the POMA program [6], assuming scalar coupling between all F atoms and an assumed single relaxation mechanism:

$$R_{2\text{F1}} = \cos(\pi J_{12}t) \cos(\pi J_{13}t) \exp(-t/T_2) \quad (6)$$

and corresponding equations for the other fluorine atoms. Here $R_{2\text{F1}}$ is the relaxation rate for the particular fluorine atom, the J_{1i} are the F–F scalar coupling constants measured from the spectra at low temperatures, T_2 is the relaxation time for the broadening mechanism, and t is the experimental time for F_1. There are similar values for the corresponding equations for the other atoms. The output equations were subjected to a Fourier Cosine Transform using Mathematica [7] and plotted for assumed values of T_2. The best simulated fits are shown in Figs. 3–5 at the temperatures indicated.
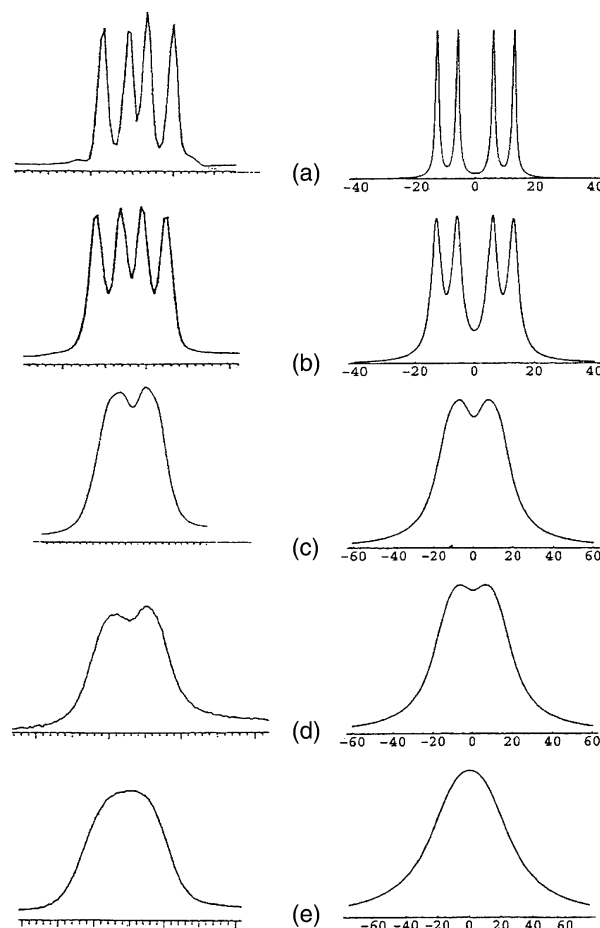

Fig. 3. Experimental (left) and calculated (right) spectra for F_1 at (a) -19, (b) -40, (c) 19, (d) 50, (e) 90 °C all at 188 MHz.

4. Discussion

The interpretation of the relaxation mechanisms for this molecule is complicated because several mechanisms are present. These are summarized in Table 1.

4.1. Spin–lattice relaxation

One of the interesting results of this work is the relatively large fraction of the spin–lattice relaxation due to chemical shift anisotropy, especially at low temperature and high field. For example at 470 MHz (11.75 T) at 220 K more than 50% of the total R_1 is due to chemical shift anisotropy. Although part of the observed shift is due to the structure of the molecule it suggests that more attention should be paid to chemical shift anisotropy not commonly measured.

Good estimates of the dipolar correlation time at each temperature can be obtained based on the assumptions described above and the relation between dipolar relaxation time and the correlation time summed over all dipolar interactions [8]:
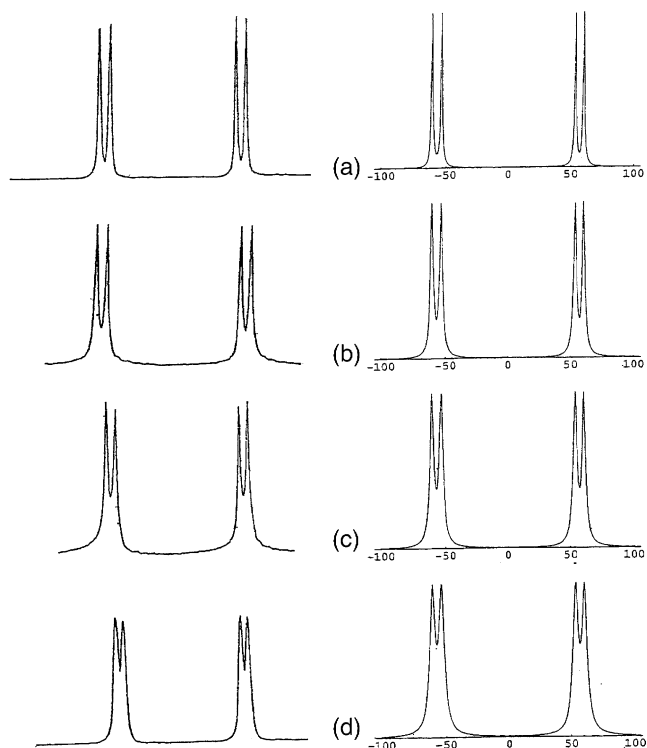
Fig. 4. Experimental (left) and calculated (right) spectra for F_2 at (a) 2, (b) 19, (c) 50, (d) 90 °C all at 188 MHz.

$$R_{1dd} = \sum 2\gamma^4 \hbar^2 \tau_{dd}/3s^6, \tag{7}$$

where γ is the magnetogyric ratio for F, $\hbar$ is Planck's constant divided by 2π, and s is the distance between the atom whose relaxation is being calculated and each of the other spin = 0 atoms in the molecule.

In the present work each F atom has only contributions to dipolar mechanism from adjacent F atoms. Thus for F_1, both F_2 and F_3 show relaxation effects while for F_2 and F_3 only F_1 is important. Based on the calculations boron was not found to make a significant contribution to dipolar relaxation to any of the F atoms. The structural distance values used were estimated values because no experimental data are available and are shown in Fig. 1. The measured spin–lattice relaxation time, $(R_1)^{-1}$, value for F_3 is noticeably longer than for the other F atoms because the distance between F_3 and F_1 is longer than the geminal distance between F_1 and F_2.

No $(R_1)^{-1}$ values for ^{11}B were measured due to their shortness.

4.2. Spin–spin relaxation

Estimates of the linewidths in Hz, R_2, for each fluorine atom at each temperature were obtained empirically by plotting the ratios of the (peak height/central dip between peaks as measured from the base line) compared to the simulated linewidth plots. Plot of $\log(R_2)$ as a function of R_2, for each of the fluorine atoms, is shown
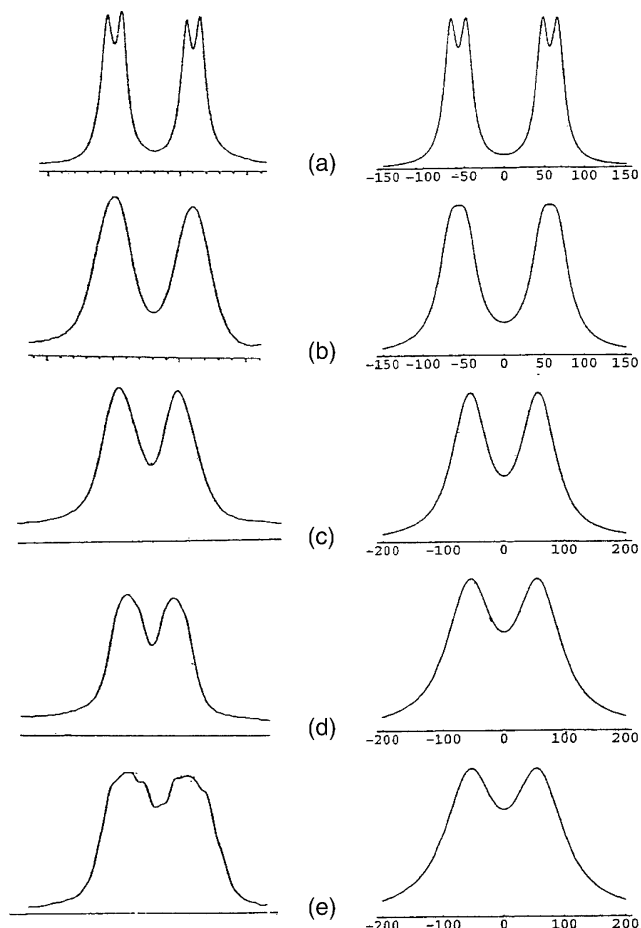

Fig. 5. Experimental (left) and calculated (right) spectra for F_3 at (a) −70, (b) −40, (c) 2, (d) 22, (e) 90 °C all at 188 MHz.

Table 1
Applicable reaction mechanisms for the various atoms

Relaxation mechanisms	Fluorine		Boron
	T_1	T_2	T_2
Dipole–dipole	X	X	X(small)
Spin–rotation	X	X	?
Chemical shift anisotropy	X	X	–
Scalar coupling	–	X	–
Quadrupolar	–	–	X

Here T_1 is the spin–lattice relaxation time and T_2 is the spin–spin relaxation time. An X indicates the mechanism is operative while a blank indicates that it is absent.

in Fig. 6 and shows only a single broadening mechanism. Also shown are the values for the boron R_2 linewidth values over the measured temperature range. The slopes of the fluorine logarithmic linewidths are nearly identical indicating the same activation energy and physical process. The slope of the boron line has a different sign showing a different relaxation process. Its linewidth decreases with increasing temperature and is due to quadrupolar relaxation. Its slight nonlinearity is
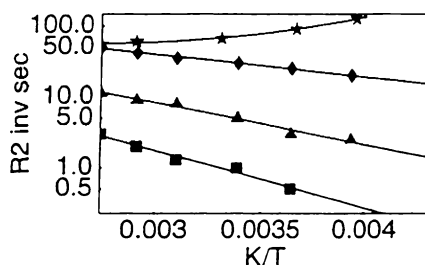
Fig. 6. Experimental log spin–spin relaxation times, R_2 for F_1 ▲, F_2 ■, F_3 ◆, and B as a function of the inverse temperature.

Fig. 7. Complete spectrum for $C_2F_3BCl_2$ at 50 °C showing both sets of peaks F_1, F_2, and F_3 from left to right. The inserts show enlargements at the base of each set.

caused by a second mechanism, possibly chemical shift anisotropy. Dipole–dipole interactions can be neglected as shown by the very small calculated interaction with the fluorine atoms.

The major spin–spin relaxation mechanism of the fluorine atoms is scalar coupling of the second kind to the boron atom. This has been treated by Abragam [8] and in more detail by others [9]. Boron relaxes rapidly due to the quadrupolar mechanism. Fluorines are coupled to the boron through the electronic structure of the molecule providing a rapid relaxation mechanism. The values of the J_{BF} scalar coupling constants can be estimated from the relation:

$$J_{BFi} = (3R_{2Fi}R_{1B}^{Q}/S(S+1))^{1/2}, \qquad (8)$$

where R_{2Fi} is the spin–lattice relaxation time for F_i, R_{1B}^{Q} is the spin–lattice relaxation time for the boron atom and $S = 3/2$ the nuclear spin for ^{11}B. In the present work the values of R_{2B}^{Q} were calculated from the linewidths and it was assumed that the R_1 and R_2 values are the same. The calculations were limited to temperatures between 253 and 363 K because at lower temperatures the boron resonance overlapped that of boron trichloride. Average values for J_{BF1}, J_{BF2}, and J_{BF3}, respectively, were found to be 71, 27, and 150 Hz.

One further observation deserves discussion. In Figs. 3–5 only a portion of the fluorine spectra are shown. In addition to the peaks shown a second identical set of peaks of low intensity occur upfield for each of the fluorine atoms. No additional low intensity fluorine peaks were observed. In Fig. 7 is shown the entire fluorine spectrum at 50 °C at 376 MHz. The small set of peaks undergoes the same scalar coupling of the second kind as the larger set observed above but with the ^{10}B isotope. Evidence for this conclusion is that the ratio of large to small peak intensity remains constant over the entire temperature range measured. If this were caused by some type of equilibrium it would require zero activation energy and is extremely unlikely. Additionally infrared spectroscopic results [10] show that the molecule is planar in solution. Theoretically the ^{11}B/^{10}B should be in the isotope occurrence ratio, i.e., 81.2/18.8. The ratios in Fig. 7 differ greatly from this and it is probably due to the differences in the T_1 values for the two isotopes. It
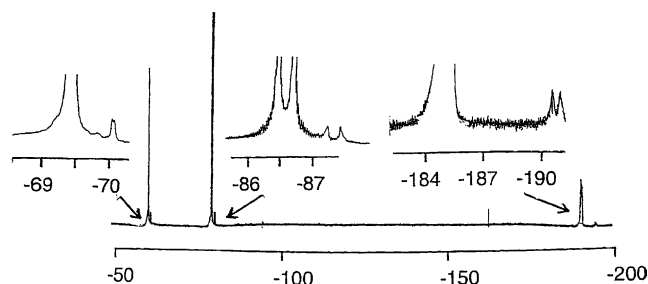
normally requires $5T_1$ between sweeps to get full peak recovery and this was probably not the case here.

Other examples of boron coupling to various nuclei have been reported in the literature. Early work has included long range B–H coupling in borazine [11] and in the carboranes [12]. Recently at least two other examples of ^{10}B splittings of fluorine peaks connected through a carbon atom have been reported. The compounds are $K[B(CF_3)_4]$ [13],[1] and $K[B(CF_3)_4COF]$ [14] and have either no or very small boron quadrupolar coupling constants due to the high structural symmetry around the boron atom. In the ^{19}F spectra of these compounds, the two sets of fluorine resonances are interspersed while in the compound reported here they are well separated. Presumably the difference between these compounds and the one studied here is connected to the symmetry of the structures.

The trifluorovinylborondichloride acidity [3] falls between that of BF_3 and BCl_3. The lower acid strength of the former is attributed to back coordination between B and the F atoms which increases the electron density on the boron and reduces its electron withdrawing ability. The larger size of the chlorine atom increases the B–Cl distance making π overlap less effective. Carbon, being a smaller atom than chlorine, would be expected to show more effective π overlap with the trifluorovinyl group showing less electron withdrawal. Coyle et al. [2] have found that the fluorine shifts for a series of trifluorovinyl metallic compounds fall in a series with the values for F_3 are always shifted to the highest field. This is in agreement with the present work where the large chemical shift anisotropy value suggests multiple bonding between the carbon and fluorine atoms.

---

[1] The authors thank one of the reviewers for calling their attention to this reference.

References

[1] H. Kaesz, S. Stafford, F.G.A. Stone, J. Am. Chem. Soc. 82 (1960) 6232.

[2] T.D. Coyle, S. Stafford, F.G.A. Stone, Spectrochim. Acta 17 (1961) 963.

[3] N. Walker, A.J. Leffler, Inorg. Chem. 13 (1974) 484.

[4] F.A. Cotton, G. Wilkinson, Advanced Inorganic Chemistry, fifth ed., Wiley Interscience, New York, 1988.

[5] E.M. Hawk, R.R.J. Sharp, J. Chem. Phys. 60 (1009) (1974) 1522.

[6] P. Guntert, N. Schaefer, G. Otting, K. Wuthrich, J. Magn. Res. A 101 (1993) 103.

[7] Mathematica, Wolfram Research Inc., Champaign, Ill.

[8] A. Abragam, The Principles of Nuclear Magnetism, Oxford Univ. Press, London, 1961.

[9] E.R. Johnson, J. Magn. Res. 60 (1984) 367;
L.G. Werbelow, A. Allouche, G. Pouzard, J. Chem. Soc., Faraday Trans. 83 (1987) 871, and earlier refs. cited.

[10] J.R. Durig, E.J. Stampf, J.D. Odom, V.F. Kalasinsky, Inorg. Chem. 16 (1977) 2895.

[11] E.K. Mellon, B.M. Coker, P.B. Dillon, Inorg. Chem. 11 (1971) 852.

[12] R.N. Grimes, Carboranes, Academic Press, New York, 1970.

[13] E. Bernhardt, G. Henkel, H. Willner, G. Pawelke, H. Burger, Chem. Eur. J. 7 (2001) 4696.

[14] M. Finze, E. Berhnhardt, H. Willner, C. Lehmann, Angew. Chem. Int. Ed. 42 (2003) 1052.